

CD8 + T cell metabolism and function are suppressed by long-chain fatty acid uptake from the bone marrow microenvironment in Multiple Myeloma

Bishop Gudgeon

University Hospitals Birmingham NHS Trust

Hannah Giles

University Hospitals Birmingham NHS Trust

Emma L Bishop

University of Birmingham

Taylor Fulton-Ward

University of Birmingham

Cristina Escribano-Gonzalez

University of Birmingham

Haydn Munford

University of Birmingham

Anna James-Bott

University of Oxford

Kane Foster

University College London

Farheen Karim

Royal Wolverhampton Hospitals NHS Trust

Dedunu Jayawardana

Royal Wolverhampton Hospitals NHS Trust

Ansar Mahmood

University Hospitals Birmingham NHS Trust

Adam Cribbs

University of Oxford

Daniel A. Tennant

University of Birmingham

Supratik Basu

Royal Wolverhampton Hospitals NHS Trust

Guy Pratt

University Hospitals Birmingham NHS Trust

Sarah Dimeloe (✉ s.k.dimeloe@bham.ac.uk)

University of Birmingham

Research Article

Keywords: Multiple Myeloma, CD8+ T cell, lipid, mitochondria, microenvironment, bone marrow

Posted Date: January 24th, 2023

DOI: <https://doi.org/10.21203/rs.3.rs-2500541/v1>

License:  This work is licensed under a Creative Commons Attribution 4.0 International License.

[Read Full License](#)

Abstract

Background

Multiple Myeloma (MM) is a plasma cell malignancy that develops in the bone marrow. Function of T lymphocytes is impaired in patients with MM and the bone marrow microenvironment is described as hostile for T cell activity. Precise suppressive mechanisms within the bone marrow microenvironment remain poorly defined but will impact efficacy of bispecific T cell engager and chimeric antigen receptor (CAR) T cell therapies.

Methods

In this study T cell phenotype, function and metabolic activity were analysed within paired bone marrow aspirate and peripheral blood samples from 72 patients across the spectrum of MM, including individuals with premalignant and asymptomatic disease, alongside age-matched controls. This permitted assessment of effects of disease stage and the bone marrow microenvironment. The bone marrow microenvironment was also modelled *in vitro* using autologous plasma co-culture systems.

Results

Bone marrow CD8⁺ T cell function decreased with MM development and was consistently lower within bone marrow samples than matched peripheral blood. These changes were accompanied by decreased mitochondrial mass, which correlated tightly with T cell function. Conversely, long-chain fatty acid uptake and peroxidation was markedly elevated in bone marrow CD8⁺ T cells. *In vitro* modelling confirmed uptake of bone marrow lipids suppresses CD8⁺ T function, which was impaired in autologous bone marrow plasma, but rescued by both lipid removal and inhibition of lipid peroxidation. Analysis of single-cell RNA-sequencing data identified expression of fatty acid transport protein 1 (FATP1) in bone marrow CD8⁺ T cells in MM, and FATP1 blockade also rescued CD8⁺ T cell function. Finally, analysis of samples from treated patient cohorts identified CD8⁺ T cell metabolic dysfunction resolves in treatment-responsive but not relapsed MM patients and is associated with substantial functional restoration.

Conclusions

CD8⁺ T cells are functionally impaired within the MM bone marrow microenvironment. This is accompanied by decreased mitochondrial mass but elevated uptake of long-chain fatty acids. Blockade of FATP1 restores CD8⁺ T cell function in presence of BM lipids and may therefore represent a novel therapeutic target to augment their activity in the bone marrow in MM and improve efficacy of T cell-directed therapies.

Background

Despite observations of T cell dysfunction in Multiple Myeloma (MM)(1–9), checkpoint blockade therapies have not been successful(10, 11), indicating that alternative suppressive mechanisms operate in the MM bone marrow (BM) microenvironment. Their identification will therefore inform novel approaches to augment anti-tumour function of endogenous and therapeutic T cells in MM.

Upon antigen recognition, T cells alter their metabolism to support clonal expansion and effector functions(12, 13). They take up more glucose and amino acids and alter metabolic pathway usage to support their anabolic effector program. Increased conversion of pyruvate to lactate enables rapid glycolytic flux, generating biosynthetic precursors. Mitochondrial biogenesis and elevated glucose and glutamine oxidation support signalling, transcription and translation through generation of reactive oxygen species (ROS), TCA cycle intermediates and ATP.

This dependence on augmented metabolism renders T cells susceptible to their microenvironment. Within solid tumours, nutrient competition limits T cell function(14–16), whilst chronic antigen exposure under hypoxia drives mitochondrial dysfunction(17, 18). Recently, immune cell lipid uptake from tumour microenvironments has been linked to loss of function. For example, in models of pancreatic ductal adenocarcinoma, melanoma and obesity-promoted breast cancer, infiltrating CD8⁺ T and NK cells accumulate long-chain fatty acids, which impair mitochondrial fitness and immune function, and can induce lipid peroxidation-driven cell death by ferroptosis(19–25). Notably, blocking lipid uptake, targeting associated transcription factors or restoring normal lipid metabolism improves immune cell function in these microenvironments.

The capacity of microenvironmental lipids to suppress T cells in MM has not been assessed but may be pertinent given the BM is a lipid rich environment, particularly in disease. Adipocytes are a major BM component, comprising up to 70% of its volume in older adults(26). Obesity increases this, and both age and obesity are independent risk factors for MM progression(27). In turn, once MM develops, MM plasma cells (MMPC) further promote adipogenesis(28) and induce BM adipocyte lipolysis, taking up released lipids to support their growth and survival(29). Consequently, T cells also encounter an enriched lipid environment in the MM BM, but the impact on their function is unknown.

In this study, we assessed T cell phenotype, function and metabolic capacity in matched peripheral blood (PB) and BM samples across the spectrum of MM, including at premalignant stages of disease and following treatment, to interrogate whether T cell metabolism is altered with MM progression and, importantly, in the MM BM microenvironment, how this relates to their function and if it can be targeted to augment T cell activity.

Materials And Methods

Patient cohort, sample collection and cell isolation

BM aspirates and PB samples were obtained from patients with monoclonal gammopathy of undetermined significance (MGUS), asymptomatic MM and MM at diagnosis, on relapse and in remission, recruited from haematology clinics at University Hospitals Birmingham and The Royal Wolverhampton Hospitals NHS Trusts (**Tables S1 and S2**). Age-matched controls were recruited from University Hospitals Birmingham NHS Trust via the Human Biomaterials Resource Centre. Control BM samples were taken from the femoral head during planned orthopaedic surgery (6/10) or following trauma (4/10). The study received ethical approval (Refs: 10/H1206/58, 20/NW/0001) and informed written consent was obtained. Mononuclear cells were isolated by density-gradient centrifugation using Ficoll-Paque (Cytiva, Cat# 17144003), harvested, washed with phosphate-buffered saline (PBS, Sigma, Cat# D8537), counted and frozen in freezing medium (10% DMSO, Sigma, Cat# 472301, 90% Foetal Calf Serum (FCS), Sigma, Cat# F9665). Plasma was frozen at -80°C.

Analysis Of Mononuclear Cells By Flow Cytometry

Mononuclear cells were thawed, washed twice in RPMI (Sigma, Cat# R8758), resuspended at 1×10^6 /ml in RPMI with 10% FCS and 100U/ml penicillin 0.1mg/ml streptomycin (Sigma, Cat# P4333) (RPMI/FCS), IL-2 (50IU/ml, Peprotech, Cat# 200-02) then rested at 37°C/5%CO₂ for 16 hours. Cells were stained for viability with efluor780 (Invitrogen, Cat# 13539140) and fluorophore-conjugated antibodies for cell surface markers (**Table S3**), together with 50nM Mitoview Green (MVG, Cambridge Bioscience, Cat# 70054), 1µM Bodipy-C₁₆ (Invitrogen Cat# D3821) or 2.5µM Bodipy 581/591 (Thermofisher, Cat #D3861) in RPMI/FCS for 20 minutes at 37°C/5%CO₂. Cells were washed twice with PBS/1% FCS and analysed using a BD LSRFortessa X-20 flow cytometer. For intracellular cytokine staining, T cells were stimulated using Immunocult CD3/28 T cell activator (StemCell, Cat# 109910) and Brefeldin A (10µg/ml, Acros organics, Cat# 297140050) for 4 hours, stained for viability and cell surface markers before fixation/permeabilization (FoxP3 buffer set, ebioscience Cat# 00-5523-00) and staining with anti-cytokine fluorophore-conjugated antibodies (**Table S3**). For CoxIV staining, cells were stimulated with T cell activator, fixed and permeabilised, stained with anti-CoxIV-AF647 (Abcam Cat# ab197491), blocked with mouse serum prior to staining for surface markers and cytokines as described. Mitochondrial mass and lipid-uptake capacity were analysed as mean fluorescence intensity (MFI) for MVG and Bodipy-C₁₆, which were normalised to the average for each batch of samples analysed concurrently. Lipid peroxidation capacity was calculated as the ratio of Bodipy 581/591 MFI at 510nm (emission after lipid peroxidation) over Bodipy 581/591 MFI at 590nm (emission before lipid peroxidation) in the same sample.

Autologous Plasma Experiments

BM mononuclear cells were thawed, washed twice in RPMI and resuspended at 1×10^6 /ml, in 50% RPMI/FCS and 50% autologous PB or BM plasma. Where indicated BM plasma was stripped of lipids using CleanAscite (Caltag, Cat# X2555-10) or additions were made: SSO (100uM, Cambridge Biosciences Cat# 11211), Ferrostatin (1uM, Selleckchem, Cat# S7243), FATP1-IN-2 (1uM, Medchem express, Cat# HY-

141700) and UDCA (ursodeoxycholic acid; 10uM, Sigma, Cat# PHR1579). T cells were stimulated for 48 hours and analysed for cell-surface marker expression, mitochondrial mass and cytokine expression by flow cytometry. Cells stained for cytokines were first stimulated for 4 hours with Cell Activation Cocktail (Biolegend, Cat#423304). Cell culture supernatants from 0.2×10^6 cells were harvested and stored at -20°C for analysis of cytokine concentration by Enzyme-linked Immunosorbent Assay (ELISA).

ELISA

IFN- γ in supernatants was measured by ELISA using anti-IFN- γ capture (Bio-Rad, Clone AbD00676, Cat# HCA043) and biotinylated detection (Bio-Rad, Clone 2503 Cat# HCA044P) antibodies, recombinant IFN- γ standard (Bio-Rad, Cat# PHP050), streptavidin-HRP (Sigma Aldrich, Cat# E2866) and TMB substrate (Bio-Rad, Cat# BUF062B). TNF- α in supernatants was measured by ELISA, using a TNF ELISA kit (Invitrogen, CHC1753 and CNB0011) according to the manufacturer's instructions.

Data Analysis

Flow cytometry data were analysed using FlowJo Version 10 (TreeStar Ltd). Statistical analysis was undertaken using Graphpad Prism Version 9.3. Statistical tests used are indicated in the figure legends.

Data Sharing

For original data please contact s.k.dimeloe@bham.ac.uk. RNA-sequencing data were accessed from GEO GSE186448 and GSE139369.

Results

Bone marrow CD8⁺ T cell function declines in Multiple Myeloma and is consistently lower than in matched peripheral blood

Phenotyping of major T cell subsets in BM and PB mononuclear cells from age-matched controls, individuals with monoclonal gammopathy of undetermined significance (MGUS), asymptomatic MM and MM at diagnosis identified that BM CD8⁺ T cell abundance decreased with disease development (**Supplementary Fig. 1A**, Fig. 1A), whilst frequencies of BM CD4⁺ T cells (Fig. 1B), as well as PB CD8⁺ and CD4⁺ T cells remained similar (**Supplementary Fig. 1B-C**). BM CD56⁺ NK cell abundance also did not change with disease development, whilst CD4⁺CD127⁻CD25⁺ regulatory T cells (TReg) were enriched in MM BM at diagnosis, agreeing with previous literature (**Supplementary Fig. 1A,D-E**)(5, 7). In PB samples, NK cells and TReg frequencies were similar at all disease stages (**Supplementary Fig. 1D,E**). We next assessed the proportion of T cells within BM and PM samples expressing the key anti-tumour cytokines interferon-gamma (IFN- γ) and tumour necrosis factor-alpha (TNF- α), as well as interleukin 2 (IL-2) and the cytotoxic molecule Granzyme B. This identified decreased frequencies of IFN- γ - and IL-2-expressing CD8⁺ T cells, as well as multifunctional CD8⁺ T cells expressing all three cytokines, and those expressing

Granzyme B in the BM with MM development (Fig. 1C). Frequencies of CD4⁺ T cells expressing these molecules did not change significantly (Fig. 1D). These observations were specific to BM CD8⁺ T cells, whilst PB T cell cytokine and granzyme expression also did not change (**Supplementary Fig. 1F-G**). Indeed, pairwise comparison of BM and PB samples identified that CD8⁺ T cells were consistently less functional within BM samples than matched PB samples. Frequencies of IFN- γ , TNF- α , IL-2- and Granzyme B-expressing CD8⁺ T cells were lower in BM than PB in all patient groups, including controls, albeit the disparity increased with disease development for IFN- γ and TNF- α . When all samples were combined, this difference was highly significant (Fig. 1E, **Supplementary Fig. 1H**). However, this was not the case for CD4⁺ T cells, which demonstrated similar functionality within BM and PB samples, and increased multifunctional cells in the BM (Fig. 1F, **Supplementary Fig. 1I**), indicating specific CD8⁺ T cell suppression within the BM microenvironment. Expression of cytokines was largely restricted to memory populations of T cells, with EMRA CD8⁺ T cells being a significant source of IFN- γ , TNF- α and Granzyme B but not IL-2 (Fig. 1G), and EM CD4⁺ T cells the major IFN- γ expressers, with contribution of CM cells for TNF- α (Fig. 1H). However, proportions of these subpopulations were broadly similar between BM and PB at all disease stages (**Figure I-J**), meaning altered overall function of CD8⁺ T cells in BM vs. PB is not explained by enrichment or loss of functionally-distinct subpopulations, and may rather relate to an effect of the microenvironment.

CD8⁺ T cell mitochondrial mass and lipid uptake alter during progression of Multiple Myeloma and in the bone marrow microenvironment

T cell function is underpinned by metabolic capacity, particularly mitochondrial mass(12, 13). Analysis of BM T cell mitochondrial mass using the fluorescent probe Mitoview Green (MVG) revealed this decreased within CD8⁺ and CD4⁺ T cells with MM development, and was reduced in MGUS, asymptomatic MM and MM at diagnosis compared to controls (Fig. 2A-B). Similar to immune effector function however, these changes were less apparent in matched PB samples (**Supplementary Fig. 2A-B**). Of note, BM CD8⁺ T cells again demonstrated significantly reduced mitochondrial mass compared to paired PB cells (Fig. 2C), which was not the case for CD4⁺ T cells (Fig. 2D), indicating a potential link between decreased mitochondrial mass and reduced functionality of CD8⁺ T cells in the BM microenvironment. To directly interrogate the relationship between mitochondrial mass and immune effector function, we stained for CoxIV, a subunit of ETC complex IV, as a mitochondrial marker, together with cytokines (since MVG cannot be fixed for intracellular staining) in a subset of samples from controls and MM at diagnosis. CoxIV expression was higher in cytokine-expressing CD8⁺ T and CD4⁺ T cells than cytokine-negative populations (Fig. 2E, **Supplementary Fig. 2D**), confirming a relationship between mitochondrial mass and effector function. In these assays, TNF- α expression was more tightly linked to CoxIV abundance than IFN- γ , potentially explained by the well-documented relationship between glycolysis and IFN- γ expression in CD8⁺ T cells(30, 31). Further confirmation that mitochondrial mass is a key determinant of T cell effector function across this patient cohort was provided by correlative analyses of MVG fluorescence vs.

frequency of cytokine expressing cells in the BM sample, which identified significant positive relationships for IFN- γ and TNF- α -expressing CD8⁺ and CD4⁺ T cells (Fig. 2F, **Supplementary Fig. 2D**).

Long-chain fatty acid uptake from tumour microenvironments is increasingly implicated in immune cell suppression through mechanisms including mitochondrial loss and dysfunction(19, 20) and lipid peroxidation-induced ferroptosis(23, 32). This may be pertinent in the lipid-rich BM, where decreased mitochondrial mass of CD8⁺ T cells was observed, therefore T cell capacity to take up long-chain fatty acids was assessed using a fluorescent palmitate probe, C₁₆-BODIPY. Uptake of this probe did not change in BM or PB T cells during disease development (Fig. 2G, **Supplementary Fig. 2E-F**) however, comparison of paired BM and PB samples revealed markedly elevated lipid uptake in BM cells, particularly CD8⁺ T cells (Fig. 2H-I, **Supplementary Fig. 2G**). Among CD8⁺ T cells, C₁₆-BODIPY uptake particularly mapped to antigen-experienced CM and EM populations and was also significantly higher in cells expressing the immune checkpoints TIGIT and PD-1 than checkpoint-negative cells (Fig. 2J). Lipid peroxidation within T cells from MM patients was also assessed using BODIPY 581/591, which fluoresces at different wavelengths before and after peroxidation. This identified that, in addition to increased lipid uptake capacity, BM T cells also demonstrate elevated lipid peroxidation than PB T cells (Fig. 2K, **Supplementary Fig. 2H**).

CD8⁺ T cell function is impaired by lipid uptake from the BM microenvironment via FATP1

Next, we established an *in vitro* model to interrogate the relationship between long-chain fatty acid uptake and T cell mitochondrial and immune dysfunction within the BM microenvironment. Specifically, we cultured BM mononuclear cells from control individuals or MM patients in autologous PB or BM plasma, stimulated T cells and assessed their mitochondrial mass and cytokine production. This established that BM plasma significantly decreased mitochondrial mass and IFN- γ expression by CD8⁺ T cells compared to PB plasma, which occurred in both control and MM samples (Fig. 3A-B). Conversely, CD4⁺ T cell mitochondrial mass was not altered in BM plasma, despite reduced IFN- γ expression (**Supplementary Fig. 3A-B**). Total secreted IFN- γ was also decreased in BM plasma cultures, as was TNF- α (Fig. 3C-D). Next, to probe a role for lipids in this suppressive activity of BM plasma, they were depleted from BM samples and compared with lipid-replete BM samples. Removal of BM lipids increased mitochondrial mass in control and MM BM CD8⁺ T cells (Fig. 3E), accompanied by restoration of IFN- γ and TNF- α expression (Fig. 3F-H). In CD4⁺ T cells however, mitochondrial mass remained unchanged, whilst IFN- γ expression was not restored (**Supplementary Fig. 3C-D**) indicating an alternative, lipid-independent mechanism of suppression, in line with the cohort data. Taken together, the data indicate that BM CD8⁺ T cells substantially take up lipids from the BM environment, leading to loss of mitochondrial mass and impaired functionality. This occurs in control BM, consistent with decreased functionality of BM vs. PB CD8⁺ T cells (Fig. 1), but may compound disease-driven loss of T cell mitochondrial mass (Fig. 2) to further compromise BM CD8⁺ T cell function in MM. To probe a role for lipid peroxidation-induced

damage in this, BM mononuclear cell cultures were treated with ferrostatin. This increased IFN- γ secretion in BM but not PB plasma (Fig. 3I-K), confirming BM lipid peroxidation contributes to T cell suppression.

Since BM lipids suppress CD8⁺ T cell function, effective blockade of relevant transporters may restore this within the BM environment. The long-chain fatty acid transporter CD36 is implicated in mediating immune-suppressive and ferroptotic effects of lipids on NK and T cell populations(19, 23). We therefore assessed its expression in BM samples and found it to be more highly expressed by CD8⁺ than CD4⁺ T cells (Fig. 3L, **Supplementary Fig. 3E**), consistent with C₁₆-BODIPY uptake data. However, analysis of cytokine expression revealed CD36-positive cells more highly expressed IFN- γ , TNF- α and IL-2 than CD36-negative counterparts, indicating activity of this transporter may not suppress BM T cell function (Fig. 7M, **Supplementary Fig. 7F**). Consistent with this, CD36 blockade did not increase CD8⁺ or CD4⁺ T cell IFN- γ expression in BM plasma (Fig. 7N, **Supplementary Fig. 7G**) and indeed decreased overall IFN- γ secreted (Fig. 7O). Therefore, to identify other relevant transporters expressed by BM CD8⁺ T cells, we explored single cell RNA-sequencing analysis of BM mononuclear cells from MM patients. Specifically, we assessed expression of the Fatty Acid Transport Proteins (FATP) 1 to 6 (SLC27A1-6). These mediate uptake of long-chain fatty acids and convert them into acyl-CoA esters, which retains them within the cell. This analysis identified that FATP1 and FATP5 are the most highly expressed family members in BM CD8⁺ T cells in MM, whilst transcripts for FATP2, 4 and 6 were scarce and for FATP3 undetectable (Fig. 3P). Analysis of control BM single cell RNA-sequencing dataset with cellular indexing of transcriptomes and epitopes by sequencing (CITE-Seq) data(33) revealed broadly similar expression patterns, with FATP1 and FATP5 being more highly expressed than FATP2, 4 or 6 (undetectable in this dataset) (**Supplementary Fig. 3H-I**). In contrast, FATP3 was more abundant in control than MM BM, yet significance of this is unclear, since FATP3 does not have confirmed lipid uptake activity(34). We therefore assessed whether blockade of FATP1 or FATP5 could restore function of CD8⁺ T cells from MM patients activated in presence of autologous BM or PB plasma. These experiments identified that specific blockade of FATP1, but not FATP5 increased T cell IFN- γ secretion (Fig. 3Q, **Supplementary Fig. 3J-K**). This did not occur in PB plasma, indicating a specific effect of BM long-chain fatty acids transported via FATP1 on CD8⁺ T cells (Fig. 7R-S). Therefore, BM long-chain fatty acids decrease CD8⁺ T cell mitochondrial mass and impair their effector function, which can be rescued by blockade of the lipid transporter FATP1.

Functional and metabolic features of CD8⁺ T cells are restored in MM patients in remission but not in relapsed patients

Finally, to understand T cell functional and metabolic phenotypes associated with poor vs. effective control of MM, we analysed samples from patients who had either relapsed on therapy or were in remission. In both groups, irrespective of treatment response, CD8⁺ T cell frequency was increased in BM and PB compared to MM patients at diagnosis (Fig. 4A, **Supplementary Fig. 4A**) and decreased CD4⁺ T cell frequency was observed (Fig. 4B, **Supplementary Fig. 4B**). Proportions of naïve, CM, EM and EMRA CD8⁺ and CD4⁺ T cell subsets were also similar between patient groups, in BM and PB (Fig. 4C-D,

Supplementary Fig. 4C-D), as were those of immune-checkpoint expressing cells (Fig. 4E-F, **Supplementary Fig. 4E-F**). However, clear differences between the two groups emerged when interrogating T cell function and metabolism, particularly within BM CD8⁺ T cell populations. Proportions of these cells expressing IFN- γ , TNF- α , IL-2 and Granzyme B were all significantly increased in patients in remission compared to those who had relapsed (Fig. 4G), as well as CD4⁺ T cells expressing IL-2 (Fig. 4H). This increased functionality was less pronounced for PB CD8⁺ T cells (**Supplementary Fig. 4G**), albeit increases in PB CD4⁺ T cell function were observed (**Supplementary Fig. 4H**). Frequency of IFN- γ , TNF- α , IL-2-expressing and multifunctional BM CD8⁺ T cells inversely correlated with malignant plasma cell abundance within aspirate samples from MM patients at diagnosis, upon relapse and in remission (Fig. 4I), supporting a role for BM CD8⁺ T cells controlling disease progression. This was also true for TNF- α , IL-2-expressing and multifunctional CD4⁺ T cells (**Supplementary Fig. 4I**). Of note, the profound restoration in BM CD8⁺ T cell function in patients in remission occurred alongside significantly decreased long-chain fatty acid uptake and increased mitochondrial mass, such that, in this group, BM and PB CD8⁺ T cell mitochondrial mass were now comparable (Fig. 6J-K). Whilst drivers of these metabolic and functional T cell changes cannot easily be determined from these cross-sectional samples from patients on diverse treatment regimens (**Table S2**), the data nevertheless highlight that effective MM control associates with specific changes in T cell metabolism, implying strategies to modulate this, such as FATP1 blockade, could be beneficial.

Discussion

In this study, analysis of T cell phenotype and function identified decreasing abundance of total and cytokine-expressing BM CD8⁺ T cell with disease progression in MM. This agrees with studies reporting diminished T cell IFN- γ expression in MM(1–3, 35) and indicates additional impairments in IL-2 and Granzyme B. Loss of T cell function during MM development may be partly explained by the corresponding loss of mitochondrial mass, which is well-described to critically underpin T cell function. In agreement, mitochondrial mass correlated with T cell cytokine expression but was decreased in MM compared to controls, and indeed in earlier disease stages. This was not observed in PB samples, indicating it is driven by the BM microenvironment, consistent with reports that chronic stimulation under hypoxia diminishes T cell respiratory capacity through suppression of PGC1- α (18). The BM microenvironment has low oxygen availability(36), likely further reduced by MMPC expansion. Another important metabolic determinant of T cell function is capacity to take up and metabolise glucose. However, assessment of T cell glucose uptake capacity was limited by lack of reliable probes(37), therefore it remains unclear if this is impacted by MM.

At all stages of disease and in control individuals, BM CD8⁺ T cells demonstrated reduced functionality compared to those in matched PB. The MM BM microenvironment is described as hostile for T cell function(38). Yet, mechanisms underpinning this remain poorly understood. Here, we observed decreased CD8⁺ T cell functionality in the BM is coupled with reduced mitochondrial mass and substantially elevated long-chain fatty acid uptake capacity. Additionally, uptake of lipids from autologous control and

MM BM plasma suppressed CD8⁺ T cell mitochondrial mass and cytokine expression, which were significantly higher in cells cultured in PB plasma or lipid-depleted BM plasma. These findings agree with accumulating studies indicating lipid uptake from tumour microenvironments impairs immune cell mitochondrial and effector function(19, 20, 23, 32). Additionally, they imply this immune-regulatory mechanism occurs even in the healthy BM niche, but that it may compound disease-driven T cell metabolic changes. Notably, CD4⁺ T cells within patient samples demonstrated lower lipid uptake and were also unaffected by BM lipids *in vitro*, despite being suppressed by BM plasma, indicating lipid-mediated suppression is restricted to CD8⁺ T cells and alternate mechanisms regulate BM CD4⁺ T cell activity.

Assessment of single cell transcriptomic data from MM patients identified BM CD8⁺ T cell expression of the long-chain fatty acid transporters FATP1 and FATP5. Additionally, FATP1 blockade restored T cell function in BM plasma, indicating it could be targeted to augment function of endogenous or therapeutic T cells in the MM BM. Notably, FATP1 blockade had little effect on T cells cultured in PB plasma, implying it targets an immunosuppressive axis unique to the BM microenvironment. Indeed, FATP1 substrates are likely enriched in the BM, an environment abundant in adipocytes(26) where local lipolysis is induced by malignant MMPC(29). MMPC also use FATP1, alongside FATP4, to acquire adipocyte-derived long-chain fatty acids, which are oxidised to support growth and treatment resistance(28, 39). Therefore, a FATP1-targeting strategy could impair malignant cell growth and augment anti-tumour immunity in MM, acting specifically within the BM microenvironmental niche. Further support for an approach to modulate T cell lipid uptake in MM is provided here by analysis of samples from patients in relapse vs. remission. Strikingly, whilst T cells in these samples were very similar in terms of abundance, phenotype and immune-checkpoint expression, the significantly improved function of T cells from patients in remission was accompanied by restored mitochondrial mass and decreased lipid uptake.

Conclusions

CD8⁺ T cells are functionally impaired within the MM bone marrow microenvironment. This is accompanied by decreased mitochondrial mass but elevated uptake of long-chain fatty acids. Blockade of the long-chain fatty acid transporter FATP1 restores CD8⁺ T cell function in presence of BM lipids and may therefore represent a novel therapeutic target to augment their activity in the bone marrow in MM and improve efficacy of T cell-directed therapies.

Declarations

Competing Interests

The authors declare no competing interests.

Acknowledgments

This work was funded by a Leukaemia UK John Goldman Fellowship and Blood Cancer UK Project Grant (21007) to SD, which also supported NG and HM. TFW was supported by a Cancer Research UK PhD Studentship. CEG and DAT are supported by a Cancer Research UK Programme Grant C42109/A24757. HG is supported by a British Society of Haematology Early-Stage Research Grant. We gratefully acknowledge the contribution to this study made by the University of Birmingham's Human Biomaterials Resource Centre, which was set up through Birmingham Science City – Experimental Medicine Network of Excellence Project.

Author Contributions

NG designed and performed research. HG, ELB, TFW, CEG, HM FK, DJ and AM collected data and performed research. AJB, KF and AC analysed and interpreted data. DAT, SB and GP designed research. SD designed and performed research, analysed and interpreted data, performed statistical analysis and wrote the manuscript.

References

1. Dhodapkar MV, Krasovsky J, Osman K, Geller MD. Vigorous premalignancy-specific effector T cell response in the bone marrow of patients with monoclonal gammopathy. *J Exp Med*. 2003 Dec 1;198(11):1753–7.
2. Fichtner S, Hose D, Engelhardt M, Meissner T, Neuber B, Krasniqi F, et al. Association of antigen-specific T-cell responses with antigen expression and immunoparalysis in multiple myeloma. *Clin Cancer Res*. 2015 Apr 1;21(7):1712–21.
3. Zelle-Rieser C, Thangavadiel S, Biedermann R, Brunner A, Stoitzner P, Willenbacher E, et al. T cells in multiple myeloma display features of exhaustion and senescence at the tumor site. *J Hematol Oncol*. 2016 Nov 3;9(1):116.
4. Goodyear O ES. Neoplastic plasma cells generate an inflammatory environment within bone marrow and markedly alter the distribution of T cells between lymphoid compartments. *Oncotarget*. 2017;8(18):30383–94.
5. Wang JN, Cao XX, Zhao AL, Cai H, Wang X, Li J. Increased activated regulatory T cell subsets and aging Treg-like cells in multiple myeloma and monoclonal gammopathy of undetermined significance: a case control study. *Cancer Cell Int*. 2018;18:187.
6. Kourelis TV, Villasboas JC, Jessen E, Dasari S, Dispenzieri A, Jevremovic D, et al. Mass cytometry dissects T cell heterogeneity in the immune tumor microenvironment of common dysproteinemias at diagnosis and after first line therapies. *Blood Cancer J*. 2019 Aug 28;9(9):72.
7. Alrasheed N, Lee L, Ghorani E, Henry JY, Conde L, Chin M, et al. Marrow-Infiltrating Regulatory T Cells Correlate with the Presence of Dysfunctional CD4(+)PD-1(+) Cells and Inferior Survival in Patients with Newly Diagnosed Multiple Myeloma. *Clin Cancer Res*. 2020 Mar 27;
8. Vuckovic S, Bryant CE, Lau KHA, Yang S, Favaloro J, McGuire HM, et al. Inverse relationship between oligoclonal expanded CD69- TTE and CD69+ TTE cells in bone marrow of multiple myeloma

- patients. *Blood Adv.* 2020 Oct 13;4(19):4593–604.
9. Bailur JK, McCachren SS, Doxie DB, Shrestha M, Pendleton K, Nooka AK, et al. Early alterations in stem-like/resident T cells, innate and myeloid cells in the bone marrow in preneoplastic gammopathy. *JCI Insight.* 2019 Apr 23;5.
 10. Lesokhin AM, Ansell SM, Armand P, Scott EC, Halwani A, Gutierrez M, et al. Nivolumab in Patients With Relapsed or Refractory Hematologic Malignancy: Preliminary Results of a Phase Ib Study. *JCO.* 2016 Aug 10;34(23):2698–704.
 11. Zanwar S, Nandakumar B, Kumar S. Immune-based therapies in the management of multiple myeloma. *Blood Cancer J.* 2020 Aug 22;10(8):84.
 12. Marchingo JM, Cantrell DA. Protein synthesis, degradation, and energy metabolism in T cell immunity. *Cell Mol Immunol.* 2022 Mar;19(3):303–15.
 13. Chapman NM, Chi H. Metabolic adaptation of lymphocytes in immunity and disease. *Immunity.* 2022 Jan 11;55(1):14–30.
 14. Ho PC, Bihuniak JD, Macintyre AN, Staron M, Liu X, Amezquita R, et al. Phosphoenolpyruvate Is a Metabolic Checkpoint of Anti-tumor T Cell Responses. *Cell.* 2015 Sep 10;162(6):1217–28.
 15. Chang CH, Qiu J, O’Sullivan D, Buck MD, Noguchi T, Curtis JD, et al. Metabolic Competition in the Tumor Microenvironment Is a Driver of Cancer Progression. *Cell.* 2015 Sep 10;162(6):1229–41.
 16. Reinfeld BI, Madden MZ, Wolf MM, Chytil A, Bader JE, Patterson AR, et al. Cell-programmed nutrient partitioning in the tumour microenvironment. *Nature.* 2021 Apr 7;1–7.
 17. Scharping NE, Menk AV, Moreci RS, Whetstone RD, Dadey RE, Watkins SC, et al. The Tumor Microenvironment Represses T Cell Mitochondrial Biogenesis to Drive Intratumoral T Cell Metabolic Insufficiency and Dysfunction. *Immunity.* 2016 Aug 16;45(2):374–88.
 18. Scharping NE, Rivadeneira DB, Menk AV, Vignali PDA, Ford BR, Rittenhouse NL, et al. Mitochondrial stress induced by continuous stimulation under hypoxia rapidly drives T cell exhaustion. *Nature Immunology.* 2021 Feb;22(2):205–15.
 19. Michelet X, Dyck L, Hogan A, Loftus RM, Duquette D, Wei K, et al. Metabolic reprogramming of natural killer cells in obesity limits antitumor responses. *Nat Immunol.* 2018 Dec;19(12):1330–40.
 20. Manzo T, Prentice BM, Anderson KG, Raman A, Schalck A, Codreanu GS, et al. Accumulation of long-chain fatty acids in the tumor microenvironment drives dysfunction in intrapancreatic CD8⁺ T cells. *J Exp Med.* 2020 Aug 3;217(8).
 21. Zhang C, Yue C, Herrmann A, Song J, Egelston C, Wang T, et al. STAT3 Activation-Induced Fatty Acid Oxidation in CD8⁺ T Effector Cells Is Critical for Obesity-Promoted Breast Tumor Growth. *Cell Metabolism.* 2020;31(1):148-161.e5.
 22. Liu X, Hartman CL, Li L, Albert CJ, Si F, Gao A, et al. Reprogramming lipid metabolism prevents effector T cell senescence and enhances tumor immunotherapy. *Science Translational Medicine.* 2021 Mar 31;13(587):eaaz6314.

23. Xu S, Chaudhary O, Rodríguez-Morales P, Sun X, Chen D, Zappasodi R, et al. Uptake of oxidized lipids by the scavenger receptor CD36 promotes lipid peroxidation and dysfunction in CD8⁺ T cells in tumors. *Immunity* [Internet]. 2021 Jun 7 [cited 2021 Jun 11]; Available from: <https://www.sciencedirect.com/science/article/pii/S1074761321002090>
24. Dyck L, Prendeville H, Raverdeau M, Wilk MM, Loftus RM, Douglas A, et al. Suppressive effects of the obese tumor microenvironment on CD8 T cell infiltration and effector function. *Journal of Experimental Medicine*. 2022 Feb 1;219(3):e20210042.
25. Prendeville H, Lynch L. Diet, lipids, and antitumor immunity. *Cell Mol Immunol*. 2022 Mar;19(3):432–44.
26. Morris EV, Edwards CM. Bone marrow adiposity and multiple myeloma. *Bone*. 2019 Jan 1;118:42–6.
27. Marinac CR, Birmann BM, Lee IM, Rosner BA, Townsend MK, Giovannucci E, et al. Body mass index throughout adulthood, physical activity, and risk of multiple myeloma: a prospective analysis in three large cohorts. *Br J Cancer*. 2018 Apr;118(7):1013–9.
28. Trotter TN, Gibson JT, Sherpa TL, Gowda PS, Peker D, Yang Y. Adipocyte-Lineage Cells Support Growth and Dissemination of Multiple Myeloma in Bone. *The American Journal of Pathology*. 2016 Nov 1;186(11):3054–63.
29. Panaroni C, Fulzele K, Mori T, Siu KT, Onyewadume C, Maebius A, et al. Multiple myeloma cells induce lipolysis in adipocytes and uptake fatty acids through fatty acid transporter proteins. *Blood*. 2022 Feb 10;139(6):876–88.
30. Chang CH, Curtis JD, Maggi LB, Faubert B, Villarino AV, O’Sullivan D, et al. Posttranscriptional control of T cell effector function by aerobic glycolysis. *Cell*. 2013 Jun 6;153(6):1239–51.
31. Gubser PM, Bantug GR, Razik L, Fischer M, Dimeloe S, Hoenger G, et al. Rapid effector function of memory CD8⁺ T cells requires an immediate-early glycolytic switch. *Nat Immunol*. 2013 Oct;14(10):1064–72.
32. Ma X, Xiao L, Liu L, Ye L, Su P, Bi E, et al. CD36-mediated ferroptosis dampens intratumoral CD8⁺ T cell effector function and impairs their antitumor ability. *Cell Metabolism* [Internet]. 2021 Mar 9 [cited 2021 Apr 29];0(0). Available from: [https://www.cell.com/cell-metabolism/abstract/S1550-4131\(21\)00071-1](https://www.cell.com/cell-metabolism/abstract/S1550-4131(21)00071-1)
33. Granja JM, Klemm S, McGinnis LM, Kathiria AS, Mezger A, Corces MR, et al. Single-cell multiomic analysis identifies regulatory programs in mixed-phenotype acute leukemia. *Nat Biotechnol*. 2019 Dec;37(12):1458–65.
34. Anderson CM, Stahl A. SLC27 fatty acid transport proteins. *Mol Aspects Med*. 2013 Apr;34(2–3):516–28.
35. Kwon M, Kim CG, Lee H, Cho H, Kim Y, Lee EC, et al. PD-1 Blockade Reinvigorates Bone Marrow CD8⁺ T Cells from Patients with Multiple Myeloma in the Presence of TGFβ Inhibitors. *Clin Cancer Res*. 2020 Apr 1;26(7):1644–55.
36. Spencer JA, Ferraro F, Roussakis E, Klein A, Wu J, Runnels JM, et al. Direct measurement of local oxygen concentration in the bone marrow of live animals. *Nature*. 2014 Apr 10;508(7495):269–73.

37. Sinclair LV, Barthelemy C, Cantrell DA. Single Cell Glucose Uptake Assays: A Cautionary Tale. *Immunometabolism*. 2020 Aug 17;2(4):e200029.
38. Manier S, Ingegnere T, Escure G, Prodhomme C, Nudel M, Mitra S, et al. Current state and next-generation CAR-T cells in multiple myeloma. *Blood Reviews*. 2022 Jan 21;100929.
39. Tirado-Velez JM, Joumady I, Saez-Benito A, Cozar-Castellano I, Perdomo G. Inhibition of fatty acid metabolism reduces human myeloma cells proliferation. *PLoS One*. 2012;7(9):e46484.

Figures

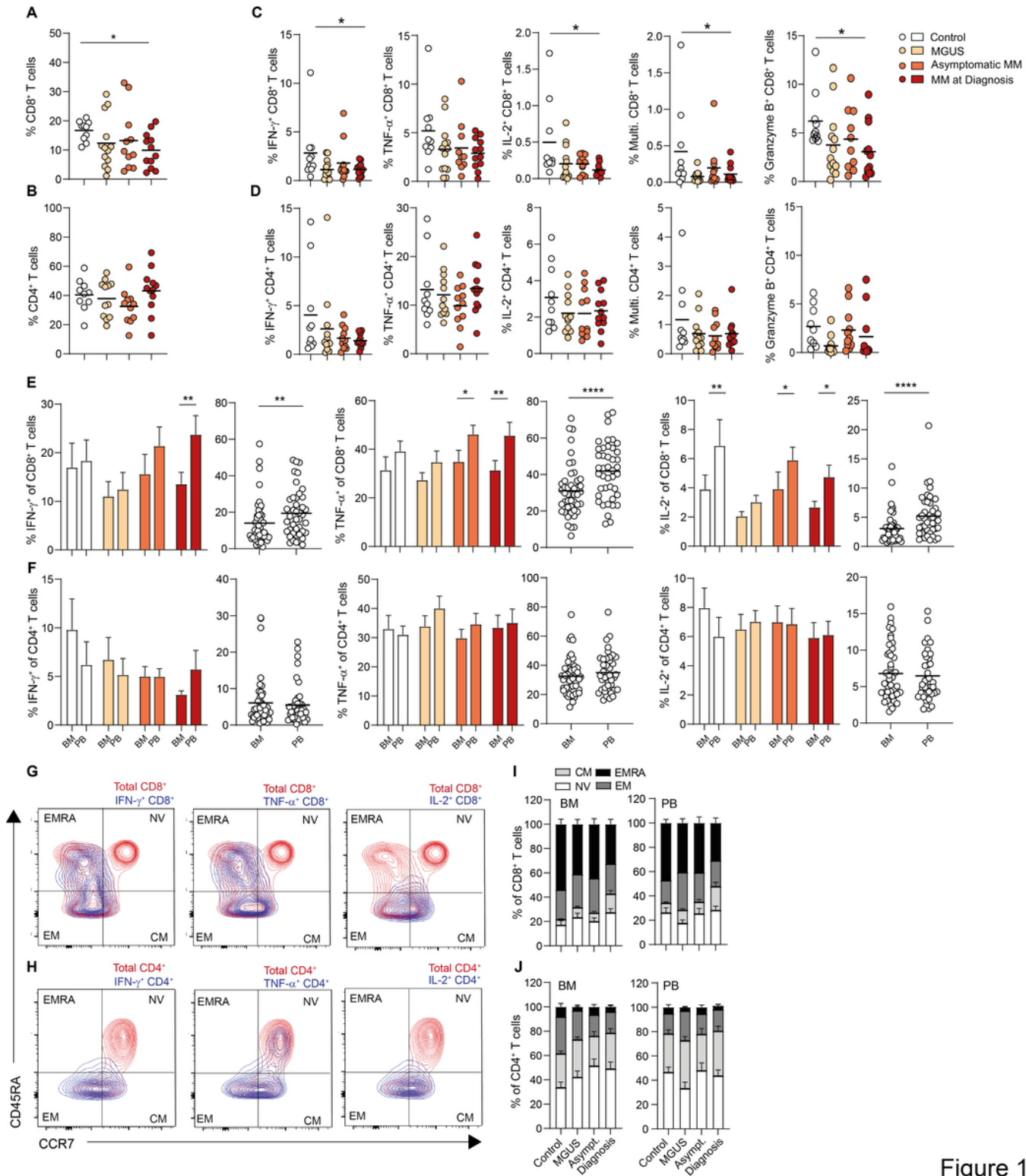


Figure 1

Figure 1

Bone marrow CD8⁺ T cell function declines in Multiple Myeloma and is consistently lower than in matched peripheral blood.

(A-B) Proportion of (A) CD8⁺ and (B) CD4⁺ T cells within bone marrow (BM) lymphocytes from controls (n=10), individuals with MGUS (n=13), asymptomatic MM (Asympt. n=11) or MM at diagnosis (Diagnosis

n=12). **(C-D)** Proportion of BM lymphocytes from indicated groups expressing **(C)** CD8 or **(D)** CD4 and IFN- γ , TNF- α , IL-2, all three cytokines (Multifunctional) or Granzyme B as indicated, after 4 hours stimulation via CD3/CD28 in presence of brefeldin A. **(E-F)** Proportion of **(E)** CD8⁺ and **(F)** CD4⁺ T cells within BM or peripheral blood (PB) lymphocytes from indicated groups expressing IFN- γ , TNF- α , or IL-2 after 4 hours stimulation as in (C-D). Proportions within the BM and PB are directly compared for each group individually and for all patients combined. **(G-H)** Representative contour plots indicate memory phenotypes of BM **(G)** CD8⁺ and **(H)** CD4⁺ T cells expressing indicated cytokine (blue) overlaid onto total populations (red). **(I-J)** Proportions of NV, CM, EM and EMRA BM and PB CD8⁺ and CD4⁺ T cells are summarised at indicated disease stages. Significance was calculated using (A, C) one-way or (E) two-way ANOVA and Holm–Sidak multiple comparison tests or (E) t test between overall paired samples; *p<0.05 **p<0.01, ***p<0.0001, ****p<0.00001.

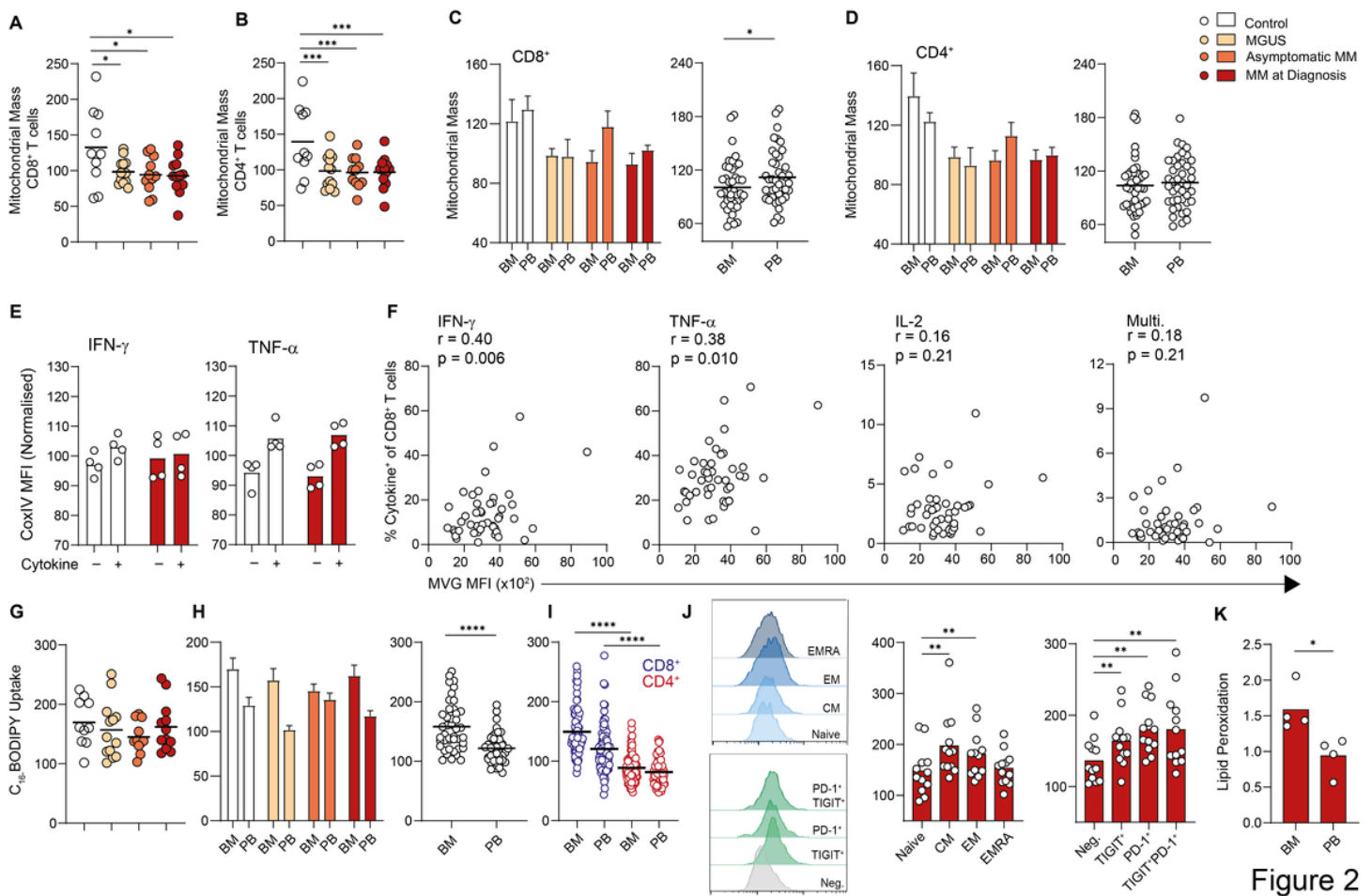


Figure 2

CD8⁺ T cell mitochondrial mass and long-chain fatty acid uptake alter during progression of Multiple Myeloma and in the bone marrow microenvironment.

(A-B) Mitochondrial mass of **(A)** CD8⁺ and **(B)** CD4⁺ T cells within BM mononuclear cells from controls (n=10), individuals with MGUS (n=13), asymptomatic MM (Asympt. n=11) or MM at diagnosis (Diagnosis

n=12) was assessed by flow cytometry using Mitoview Green (MVG) and is expressed relative to the mean of each experiment. **(C-D)** Mitochondrial mass of BM and PB CD8⁺ and CD4⁺ T cells is directly compared for each group and for all patient samples combined. **(E)** CoxIV MFI of CD8⁺ T cells positive or negative for IFN- γ or TNF- α as indicated from control (n=4) or MM at diagnosis (n=4) samples. **(F)** Correlation of mitochondrial mass (MVG fluorescence) with frequency of BM CD8⁺ T cells positive (+) for the indicated cytokines for all patient samples combined. **(G)** C₁₆-BODIPY uptake of BM CD8⁺ T cells within indicated groups expressed relative to the mean of each experiment. **(H)** C₁₆-BODIPY uptake of BM and PB CD8⁺ T cells is directly compared for each group and for all patient samples combined. **(I)** C₁₆-BODIPY uptake of BM and PB CD8⁺ and CD4⁺ T cells directly compared for all patients combined. **(J)** C₁₆-BODIPY uptake of **(J)** naïve (NV), central memory (CM) effector memory (EM) and EMRA BM CD8⁺ T cell subsets and subsets expressing TIGIT and/or PD-1 as indicated from samples with MM at diagnosis (n=12). **(K)** Lipid peroxidation capacity of CD8⁺ T cells within BM and PB mononuclear cells from MM patients at diagnosis (n=4), assessed using the lipid peroxidation probe Bodipy 581/591. Significance was calculated using **(A, I-J)** one-way ANOVA and Holm–Sidak multiple comparison tests, **(C,H,K)** paired t test, **(F)** Pearson correlation ; *p<0.05, **p < 0.01, ***p < 0.0001, ****p < 0.00001.

(left) and both combined (right). **(B)** At 72 hours T cells were activated with PMA/ionomycin and expression of IFN- γ was assessed within CD8 $^{+}$ T cells by flow cytometry. **(C-D)** IFN- γ and TNF- α in cell culture supernatants was measured by ELISA. **(E-H)** BM mononuclear cells were cultured and assessed as in **(A-D)** but in either complete or lipid-depleted BM autologous plasma as indicated. **(I-K)** BM mononuclear cells from MM patients at diagnosis (n=6) were cultured in autologous PB **(I,K)** or BM **(J,K)** plasma as in **(A-D)**, in absence or presence of Ferrostatin and assessed for IFN- γ expression by ELISA. **(L)** Proportion of CD8 $^{+}$ T cells expressing CD36 within indicated BM mononuclear cell samples from controls (n=10), individuals with MGUS (n=8), asymptomatic MM (Asympt. n=9) or MM at diagnosis (Diagnosis n=7) were assessed by flow cytometry. **(M)** Expression of IFN- γ , TNF- α and IL-2 by CD36 positive and negative CD8 $^{+}$ T cells within indicated BM mononuclear cell samples as in **(L)** **(N-O)** BM mononuclear cells from MM patients at diagnosis (n=7) were cultured in autologous BM plasma as in **(A-D)**, in absence or presence of the CD36 inhibitor, SSO and assessed for IFN- γ expression within CD8 $^{+}$ T cells by flow cytometry **(N)** or by ELISA **(O)**. **(P)** sc-RNA-seq UMAP projections of BM mononuclear cells from MM patients at diagnosis, with cell type annotation (top left) and transcript abundance of indicated genes overlaid. **(Q-S)** BM mononuclear cells from MM patients at diagnosis (n=7) were cultured in autologous PB **(Q,S)** or BM **(R,S)** plasma as in **(A-D)**, in absence or presence of the FATP1 inhibitor FATP1in2 and assessed for IFN- γ expression by ELISA. Significance was calculated using **(A-H)** Mann-Whitney or **(K,S)** paired t test; *p<0.05, **p < 0.01, ***p < 0.0001.

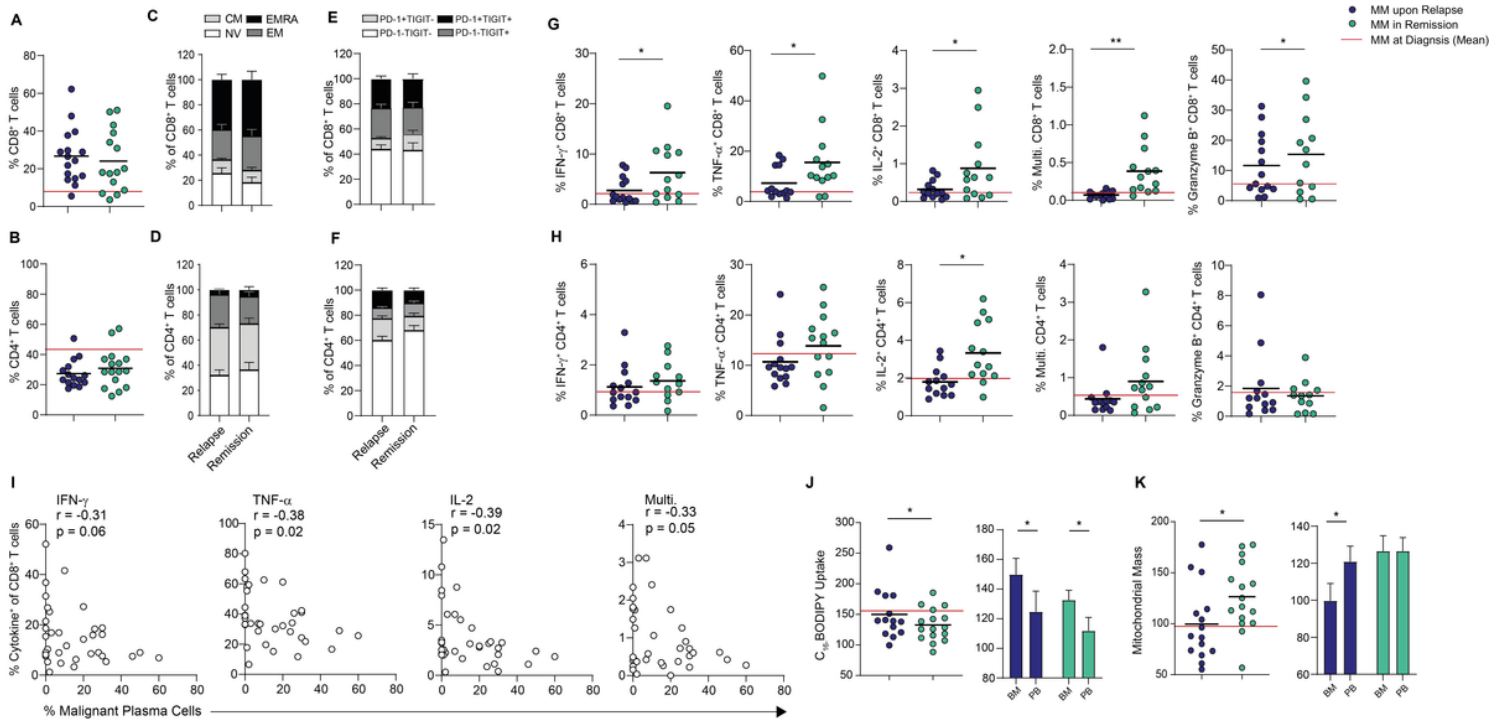


Figure 4

Figure 4

Functional and metabolic features of CD8 $^{+}$ T cells are restored in Multiple Myeloma patients in remission but not in relapsed patients

(**A-B**) Proportion of (**A**) CD8⁺ and (**B**) CD4⁺ T cells within bone marrow (BM) mononuclear cells from relapsed MM patients (n=14) and MM patients in remission (n=12). (**C-D**) Proportions of NV, CM, EM and EMRA (**C**) CD8⁺ and (**D**) CD4⁺ T cells in indicated BM samples. (**E-F**) Percentage of PD-1⁻TIGIT⁻, PD-1⁺TIGIT⁻, PD-1⁻TIGIT⁺ and PD-1⁺TIGIT⁺ (**E**) CD8⁺ and (**F**) CD4⁺ T cells in BM mononuclear cells from indicated samples. (**G-H**) Proportion of (**G**) CD8⁺ and (**H**) CD4⁺ T cells within BM mononuclear cells from each group expressing IFN- γ , TNF- α , IL-2, all three of these cytokines (Multifunctional) or Granzyme B after 4 hours of stimulation via CD3/CD28 brefeldin A. (**I**) Correlation of percentage of malignant plasma cells within the BM sample with frequency of cells positive (+) for the indicated cytokines for samples combined for patients with MM at diagnosis (n=12), relapsed MM patients (n=14) and MM patients in remission (n=12). (**J**) C₁₆-BODIPY uptake and (**K**) mitochondrial mass of BM and PB CD8⁺ T cells within each group as indicated. The red line indicates the mean value in MM patients at diagnosis. Significance was calculated using (**G-H, J-K**) unpaired t test (**J**) two-way ANOVA and Holm–Sidak multiple comparison tests and (**I**) Pearson correlation; *p<0.05, **p < 0.01.

Supplementary Files

This is a list of supplementary files associated with this preprint. Click to download.

- [SupplementCD8MMJH0.docx](#)